Quest: Journal of Geometry, Mathematical and Quantum Physics (Quest)

e-ISSN: 3064-7282 Vol.3 Issue 9|2026

Study of Fusion and Breakup Reactions of Some Nuclei

Malik S. Mhaimeed[1]

1. Open Education College, Education Directorate Babylon, Ministry of Education, Babil, Iraq

*Correspondence: Malksalh455@gmail.com

Citation: Mhaimeed, M. S. Study of Fusion and Breakup Reactions of Some Nuclei. Quest: Journal of Geometry, Mathematical and Quantum Physics (Quest) 2026, 3(9), 1-7.

Received: 6th June 2026
Revised: 11th July 2026
Accepted: 15th August 2026
Published: 4th September 2026

Abstract: A study was conducted utilizing coupled-channel calculations to investigate the fusion cross-section (σ_{fus})and fusion-barrier distribution (D_{fus}) for the nuclear systems ^{23}Na + ^{40}Ca, ^{28}Si + ^{64}Ni, and ^{19}F + ^{54}Fe. This investigation employed the semiclassical method and Wong formula. The semiclassical method was primarily utilized to address Coulomb excitation effects within the nucleus. Fusion barrier distributions were determined experimentally and theoretically using the three-points method. A comparison between theoretical predictions and experimental data revealed significant agreement for the 6Li+64Ni and 124Sn+48Ca systems. However, discrepancies were observed for the 40Ca+96Zr system both below and above the Coulomb barrier (V_b).

Keywords: Fusion, breakup, nuclei

1. Introduction

The investigation of nuclear fusion represents a highly intriguing and extensively researched phenomenon within the scientific community. Its study is pivotal due to its implications for the synthesis of super heavy nuclei and the comprehension of astrophysical nucleosynthesis. The collision between two nuclei can instigate diverse processes, traditionally categorized in a semiclassical framework as either compound nucleus reactions, associated with fusion reactions, or direct reactions, differentiated by the impact parameter or relative angular momentum. The former predominates in interactions of a more central nature, where the impact parameter aligns with the grazing trajectory. Intermediate activities manifest as deep and inelastic reactions. Various factors, notably kinetic energy and the consequential Coulomb repulsion, significantly influence the prevalence of these mechanisms [1, 2].

The Coulomb sub-barrier height surpasses the kinetic energy, leading to a departure from the previous notion of independence; the interrelation of processes is now recognized as integral. This interconnectedness is exemplified in the coupling of distinct reaction channels, as delineated in the principle of diffusion [3]. The comprehensive wave function governing the scattering conundrum encompasses not only the initial channel but also all potential exit channels, with the Hamiltonian incorporating pertinent potential terms like the exciting potential. Our earlier research delved into the examination of coupled channels using both semiclassical and full quantum mechanical frameworks across diverse systems, showcasing notable success, notably in refining the determination of fusion cross-section (σ_{fus}) below the Coulomb barrier (V_b). Interested readers are encouraged to consult our previously published studies for further insights [4].

The primary objective of the present investigation is to scrutinize the impact of incorporating coupling effects on fusion reaction calculations of σ_{fus} and D_{fus}, for the reaction systems $^{23}Na + ^{40}Ca$, $^{28}Si + ^{64}Ni$, and $^{19}F + ^{54}Fe$. The selected semiclassical methodology predominantly addresses the treatment of Coulomb excitation within the nucleus. To validate our theoretical projections, fusion barrier distributions will be ascertained experimentally and theoretically, employing the three-point method to compare against empirical data [5].

2. Materials and Methods

The semiclassical approach, previously employed to investigate fusion reactions within a single-barrier potential model, considers the relative motion of colliding heavy ions as an unrestricted parameter. This theory delves into the Schrödinger equation, encompassing independent angular momentum and energy terms, alongside the energy potential concerning relative motion coordinates and the radial component involving quantum tunneling phenomena. The equation at the core of this theory is depicted as follows [6]:

$$[-\hbar^2\nabla^2/2\mu + V(r) - E]\,\psi(r) = 0 \qquad (1)$$

In the context of the system under consideration, the symbol V(r) denotes the potential of the system, while μ signifies the reduced mass of the system. Equation 1's wave functions can be approximated by solving the time-dependent Schrödinger equation, with the assumption that the particle's path follows the classical Rutherford trajectory. This trajectory incorporates both the real component of the Coulomb potential and the centrifugal potential, as described in reference [7].

$$V(r) = V_C(r) + V_N(r) + V_\ell(r) \qquad (2)$$

The incorporation of the imaginary component of the nuclear potential is essential in coupled-channel calculations to address significant absorption effects in regions traditionally inaccessible according to classical mechanics, particularly in the context of elastic channel scattering [8].

$$V_N(r) = U_N(r) - iW(r) \qquad (3)$$

The utilization of wave expansion techniques has been applied in the examination of pronounced absorption resulting from the interference of angular momentum waves stemming from the interplay between the actual and imaginary components of the nuclear potential [9]. As indicated by semiclassical principles, the fusion reaction occurs as two atomic nuclei approach each other, surmounting the potential barrier into the inner region. Subsequently, the likelihood of penetration below the barrier can be calculated using the Wentzel – Kramers - Brillouin (WKB) method [10].

$$P_{fus}^{WKB}(\ell, E) = \frac{1}{1 + e^{\left(2\int_{r_b^{(\ell)}}^{r_a^{(\ell)}} \kappa_\ell(r)dr\right)}} \qquad (4)$$

The local wavefunction number denoted as $\kappa_l(r)$ is characterized by the boundaries $r_a^{(l)}$ and $r_b^{(l)}$ corresponding to the classical trajectory's inflection points, leading to the formulation of equation 4.

$$P_{fus}^{WKB}(\ell, E) = \frac{1}{1 + e^{\left(\frac{2\pi}{\hbar\Omega_\ell}(V_b(\ell) - E)\right)}} \qquad (5)$$

Given that the fusion barrier conforms to a parabolic shape, the likelihood of penetration can be elucidated using the Hill-Wheeler formula as indicated in reference [11].

$$P_{fus}^{WH}(\ell, E) = \frac{1}{1 + exp\left[\frac{2\pi}{\hbar\Omega_l}\left(E - V_b(\ell)\right)\right]} \qquad (6)$$

The parameters Ω_l and $V_b(l)$ represent the curvature and height of the barrier utilized in the determination of the fusion barrier, respectively, while E denotes the energy of the projectile striking the target. The application of the WKB approximation allows for the computation of the fusion cross-section through the utilization of the equations provided [12,13].

$$\sigma_{fus}(E) = \frac{\pi}{\kappa^2}\sum(2\ell+1)P_{fus}^{WKB}(\ell, \quad E) \tag{7}$$

$$P_{fus}^{\gamma}(\ell, E) = \frac{4k}{E}\int \left|u_{\gamma\ell}(k_\gamma, r)\right|^2 W_{fus}^{\gamma}(r)\, dr \tag{8}$$

The function $W_{fus}^{\gamma}(r)$ represents the imaginary potential component, while $u_{\gamma l}(k_\gamma, r)$ signifies the radial segment of the wave function corresponding to the partial-wave ℓ in the γ-channel. The theoretical framework of the semiclassical approach applied in the analysis of heavy ion fusion involves considerations of degrees of freedom, classical trajectory motion r, and intrinsic characteristics of the projectile denoted by ζ. The resulting coupled-channel Hamiltonian can be expressed as such [14]:

$$h = h_0(\zeta) + V(\zeta, r) \tag{9}$$

The formula $V(\xi, r) = V_C(\zeta, r) + V_N(\zeta, r)$ is utilized, with $h_0(\zeta)$ representing the Hamiltonian pertaining to the intrinsic states, and $V(\xi, r)$ denoting the interaction between the target and projectile. Rutherford's trajectory theory establishes a connection between the collision energy, E, and the angular momentum, l. The resolution to the classical equation $V(r) = \langle\psi_0|V(r,\zeta)|\psi_0\rangle$ is sought, where ψ_0 signifies the ground state of the projectile. Given the time-dependent nature of the interaction, $V_l(\xi.t) = V(r_{l(t)}, \zeta)$ is considered, and the intrinsic eigenstates of the Hamiltonian are governed by the Schrödinger equation [15,16].

$$h|\Psi_\gamma\rangle = \varepsilon|\Psi_\gamma\rangle \tag{10}$$

Regarding the foundational aspect, the wave function's expansion is subsequently articulated [17].

$$\psi(\zeta, t) = \sum a_\gamma(\ell, t)\psi_\gamma(\zeta)e^{-i\varepsilon_\gamma t/\hbar} \tag{11}$$

Upon inserting equation (11) into equation (10), the system of Alder-Winther coupled equations is obtained [18].

$$i\hbar\, \dot{a}_\gamma(l, t) = \sum_{\epsilon}\langle\psi_\gamma|V(\zeta, t)|\psi_\gamma\rangle\, e^{i(\varepsilon_\gamma - \varepsilon_\epsilon)t/\hbar}\gamma\epsilon(l, t) \tag{12}$$

The establishment of initial conditions $a_\gamma(\ell, t \to -\infty) = \delta_{\gamma 0}$ is crucial for the resolution of the interconnected differential equations at the asymptotic limit (t→-∞), determining the fusion probability $P_{fus}^{\gamma}(\ell, E) = \left|a_\gamma(\ell, t \to -\infty)\right|^2 of\, \gamma$ for the final population in the γ-channel [19].

Determining the parameter D_{fus}, which represents the fusion barrier distribution, is a highly sensitive task as defined in previous studies [20,21].

$$D_{fus}(E) = \frac{d^2\mathcal{F}(E)}{dE^2} \tag{13}$$

The symbol $F(E)$ denotes the fusion barrier distribution function.

$$\mathcal{F}(E) = E\sigma_{fus}(E) \tag{14}$$

The experimental determination of the distribution of the fusion reaction barrier has significantly advanced the comprehension of fusion reactions. The uncertainties associated with numerical calculations of this barrier can be assessed through the reaction [22,23].

$$D_{fus}(E) \cong \frac{\mathcal{F}(E+\Delta E) + \mathcal{F}(E-\Delta E) - 2\mathcal{F}(E)}{\Delta E^2} \tag{15}$$

In this context, the range is denoted as ΔE around every recorded cross-sectional data point corresponding to excitation energy. Subsequently, the statistical uncertainty is calculated using the formula [24,25].

$$\delta D_{fus}^{stat}(E) \approx \frac{\sqrt{[\delta\mathcal{F}(E+\Delta E)]^2 + [\delta\mathcal{F}(E-\Delta E)]^2 + 4[\delta\mathcal{F}(E)]^2}}{(\Delta E)^2} \tag{16}$$

The uncertainty $\delta F(E)$ represents the multiplication of $E\sigma_f)$ for every collision energy, as indicated in reference [26].

$$\delta D_{fus}^{stat}(E) \cong \frac{\sqrt{6}\delta\mathcal{F}(E)}{(\Delta E)^2} \tag{17}$$

3. Results and Discussion

The semiclassical and the full quantum mechanical calculations have been performed by using by using spatial codes. The Nuclear potential is taken to be of Woods-Saxon potential. The Woods-Saxon parameter for the Akyu¨z-Winther potential V0, r0 and a0, were determined using a least-squares method to the experimental data of fusion cross sections by distribution barrier FDFP. These potential parameters were used for both semiclassical and full quantum mechanical calculations. The optical potential parameters of the Woods-Saxon potential were also estimated by fitting to the experimental data of the barrier height V_b. The fusion barrier distribution D_f has been calculated by using the numerical Three Point Difference Method (TPDM) for QMCC code, while for SCF code Wong fit has been used along with the TPDM. These parameters are listed in Table I.

Table 1. The Akyüz-Winther potential parameters.

Parameter	**^{23}Na + ^{40}Ca**	**^{28}Si + ^{64}Ni**	**^{19}F + ^{54}Fe**
Real Part — V(r)			
V_0 (MeV)	**54.69**	**60.20**	**54.97**
R_o (fm)	**7.337**	**9.988**	**9.135**
a_v (fm)	**0.63**	**0.63**	**0.63**
R_1 proj (fm)	**3.323**	**3.554**	**3.112**
R_2 targ (fm)	**4.014**	**4.710**	**4.446**
Imaginary Part — W(r)			
W_0 (MeV)	**42.66**	**46.95**	**42.87**
$R^W = R_0$ (fm)	**7.337**	**9.988**	**9.135**
a^W (fm)	**0.63**	**0.63**	**0.63**
W_o/V_0	**0.78**	**0.78**	**0.78**
Barrier & Fit Parameters			
V_b (MeV)	**43.181**	**54.016**	**35.256**
ħω (MeV)	**2.143**	**4.839**	**5.032**
r_0 (fm)	**1.171**	**1.419**	**1.417**
r^c (fm)	**8.143**	**9.148**	**8.383**
μ (MeV/c²)	**13602.9**	**18144.0**	**13092.0**
χ^2/N	**—**	**361.67**	**1667.44**
Method	**AW nominal**	**best-fit**	**best-fit**

3-1 ^{23}Na + ^{40}Ca system

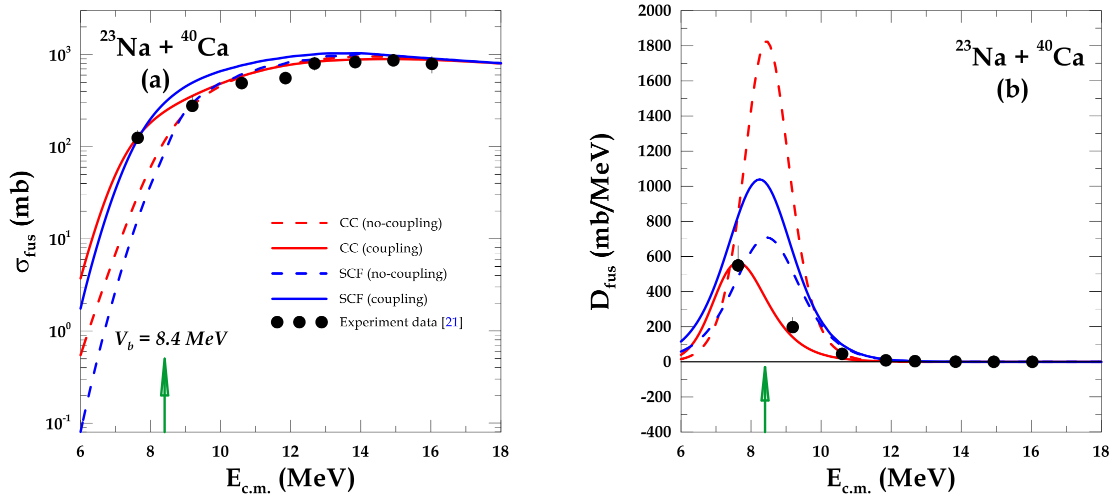

Figure 1. The comparison between semiclassical and full quantum mechanical calculations with the experimental data for **^{23}Na + ^{40}Ca** system. Panel (a) for the total fusion cross section σ_f

$_{us}$ (mb), panel (b) for the fusion barrier distribution D_{fus} (mb/MeV).

(a) Fusion Cross Section σ_{fus} (mb)

The cross section increases sharply near the barrier energy (~5–7 MeV region). The experimental data points (black circles) lie above the no-coupling calculation at sub-barrier energies.

This indicates strong enhancement of fusion probability below the barrier and significant coupling effects.

The coupled-channels calculations provide a much better fit to experimental data, demonstrating that nuclear excitations strongly influence the reaction dynamics.

(b) Barrier Distribution D_{fus} (mb/MeV).

The barrier distribution plot shows a broad structure rather than a single sharp peak where the multiple components indicating coupling to internal states.

The no-coupling calculation produces a narrow, high peak. In contrast, the coupled calculations reproduce the experimental spread, confirming that barrier distribution broadening results from channel coupling.

3-2 ^{28}Si + ^{64}Ni system

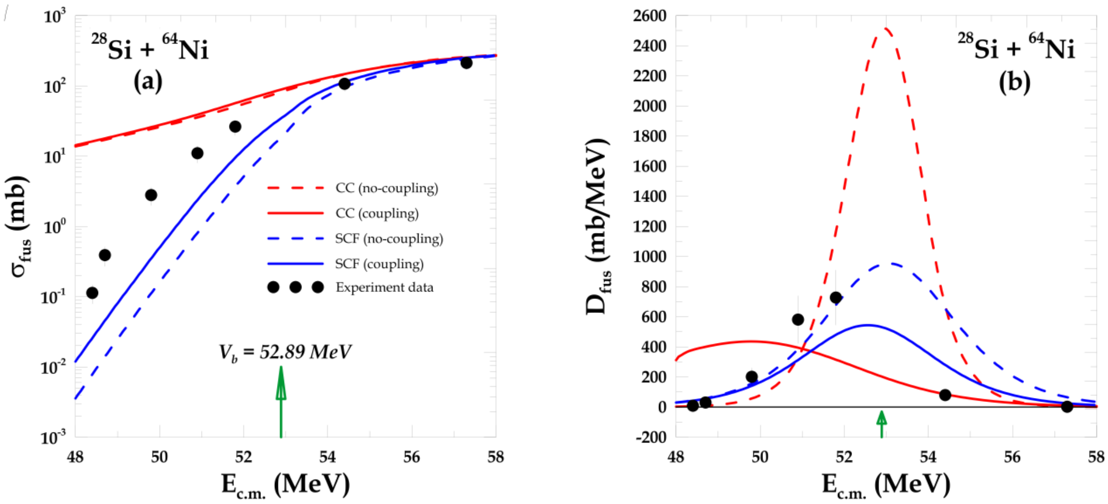

Figure 2. The comparison between semiclassical and full quantum mechanical calculations with the experimental data for ^{28}Si + ^{64}Ni system. Panel (a) for the total fusion cross section σ_{fus} (mb), panel (b) for the fusion barrier distribution D_{fus} (mb/MeV).

(a) Fusion Cross Section

The experimental cross sections show clear sub-barrier enhancement deviation from single-barrier predictions

The coupled-channels models significantly improve agreement, particularly below the barrier (around 52–55 MeV). This suggests collective excitations in ^{28}Si and/or ^{64}Ni strong deformation effects.

(b) Barrier Distribution

The barrier distribution exhibits a pronounced multi-peak structure, greater width compared to the lighter system, this indicates stronger coupling and more complex nuclear structure effects.

The broader distribution confirms that the fusion process is influenced by multiple reaction pathways.

3-3 ^{19}F + ^{54}Fe system

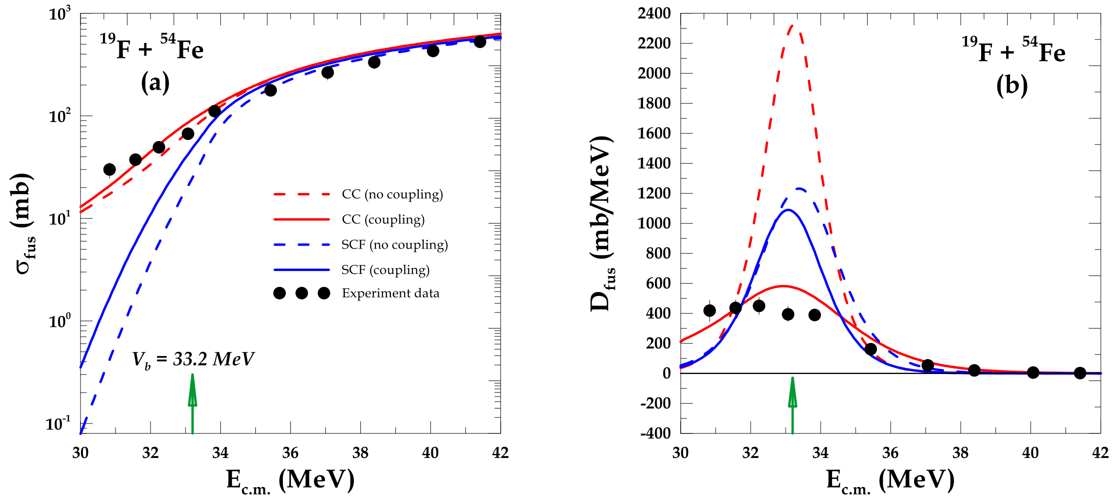

Figure 3: The comparison between semiclassical and full quantum mechanical calculations with the experimental data for ^{19}F + ^{54}Fe system. Panel (a) for the total fusion cross section σ_{fus} (mb), panel (b) for the fusion barrier distribution D_{fus} (mb/MeV).

(a) Fusion Cross Section

The experimental data show smooth increase with energy, noticeable sub-barrier enhancement

Again, the no-coupling calculation underestimates sub-barrier fusion. Coupled-channels calculations closely reproduce experimental results, confirming the importance of vibrational or rotational couplings.

(b) Barrier Distribution

The barrier distribution shows a moderately broad peak, reduced sharpness compared to the no-coupling prediction.

The experimental distribution aligns better with coupled models, demonstrating that internal nuclear dynamics significantly modify the effective fusion barrier.

4. Conclusion

The comparative analysis of the three systems emerge: 4-1 For the sub-barrier Enhancement. All experimental data exceed the no-coupling predictions below the barrier. 4-2 For the barrier Broadening. Experimental barrier distributions are broader and multi-peaked. 4-3 For the importance of Nuclear Structure Systems involving deformed or collective nuclei show stronger coupling effects. 4-4 For the model Validation. Coupled-channels calculations consistently improve agreement with experimental results.

REFERENCES

[1] C. A. Bertulani and P. Danielewicz, Introduction to nuclear reactions (CRC Press, 2004

[2] P. J. Siemens, Lett. Nat. 305, 410 (1983).

[3] R. J .Glauber,. Phys. Rev. 100, 242 (1955).

[4] C. Y. Wong, Phys. Rev. Lett. 31, 766 (1973).

[5] G.R Satchler, Introduction to Nuclear Reactions. 2nd ed, MacMillan Education Ltd, London, 1990.

[6] F. A. Majeed, R. Sh. Hamodi, and F. M. Hussian. Advanced Studies in Theoretical Physics 11, 415-427(2017)

[7] F. A. Majeed, K. H.H. AlAteah and M. S. Mehemed. Int.J.Energ.Sci. Tech, 11, 291-308(2018).

[8] M. Beckerman, Phys. Rep. 129, 145 (1985).
[9] F.A. Majeed, Y.A. Abdul-Hussien. J. Theor, App. Phys. 107, 1 (2016).
[10] F.A. Majeed. Int. J. Nucl. Energ. Sci. Tech. 11, 218 (2017).
[11] F. A. Majeed, R. Sh. Hamodi, F. M. Hussian. J. Comput.Theor. Nanosci. 14, 2242 (20017).
[12] F. A.Majeed, Khalid HH AlAteaH, and Malik S. Mhaimeed. J. of Kufa-phys. 10, 68-77(2018).
[13] F. A. Majeed, and F. A. Mahdi. Ukrain. Jour. of Phys. 64, 11-11 (2019).
[14] F. A. Majeed, Y. A. Abdul-Hussien, and F. M. Hussian. "Fusion Reaction of Weakly Bound Nuclei." In Nuclear Fusion-One Noble Goal and a Variety of Scientific and Technological Challenges. IntechOpen (2019).
[15] A. J. Najim, F. A. Majeed, and Kh. H. Al-Attiyah. In IOP Conference Series: Materials Science and Engineering, vol. 571, 012124. IOP Publishing (2019).
[16] A. J. Najim, F. A. Majeed and Khalid H. A. Al-Attiyah, J. of Eng. and Appl. Sci. 14. 10406-10412(2019.)
[17] F. M. Hussain, F. A. Majeed, and Y. A. Abdul-Hussien. In AIP Conference Proceedings, 2144, 030003. AIP Publishing LLC (2019).
[18] F. M. Hussain, F. A. Majeed, and Abdul-Hussien, Y. A. In IOP Conference Series: Materials Science and Engineering. 571. 012113. IOP Publishing (2019).
[19] C. A. Bertulani, and L. F. Canto. Nucl. Phys. A 539, 163-176 (1992).
[20] P. Gomes, T. Penna, E. Chagas, R. L. Neto, J. Acquadro, P. Pascholati, E. Crema, C. Tenreiro, N. C. Filho, and M. Coimbra. Nucl. Phys. A 534. 429(1991).
[21] M. S. Hussein, M. P. Pato, L. F. Canto, and R. Donangelo. Phys.Rev. C 47, 2398-2400(1993).
[22] W.H.Z. Cárdenas, L.F. Canto, R., Donangelo, M.S. Hussein, Lubian, J., Romanelli, A. Nucl. Phys. A703. 633–648(2002).
[23] F. A. Majeed, F. M. Hussain, and Y. A Abdul-Hussien. International Journal of Nuclear Energy Science and Technology, 13(3), 226-241(2019).
[24] L. F. Canto, R. Donangelo, and H. D. Marta. Phys. Rev. C73. 034608 (2006).
[25] K. Alder, A. Winther, "Electromagnetic Excitations", North- Holland, Amsterdam (1975).
[26] P. R. S. Gomes, M. D. Rodríguez, G. V. Martí, I. Padron, and L. C. Chamon. Phys. Rev. C 71, 034608 (2005).